Martensitic transformation and giant magnetic entropy change in $Ni_{42.8}Mn_{40.3}Co_{5.7}Sn_{11.2}$ alloy*

Chen Feng-Hua(陈峰华)[a)c)], Gong Chang-Wei(宫长伟)[b)], Guo Yan-Ping(郭艳萍)[b)], Zhang Min-Gang(张敏刚)[b)†], and Chai Yue-Sheng(柴跃生)[b)]

[a)] College of Mechanical Engineering, Heavy Machinery Engineering Research Center of Ministry of Education of China, Taiyuan University of Science and Technology, Taiyuan 030024, China

[b)] College of Materials Science and Engineering, Taiyuan University of Science and Technology, Taiyuan 030024, China

[c)] Department of Physics, School of Applied Science, Taiyuan University of Science and Technology, Taiyuan 030024, China

(Received 22 September 2013; revised manuscript received 8 December 2013; published online 10 April 2014)

The crystal structure, phase transition, and magnetocaloric effect in $Ni_{42.8}Mn_{40.3}Co_{5.7}Sn_{11.2}$ alloy are investigated by structure analysis and magnetic measurements. A large magnetic entropy change of 45.6 J/kg·K is obtained at 215 K under a magnetic field of 30 kOe (1 Oe = 79.5775 A·m^{-1}). The effective refrigerant capacity of $Ni_{42.8}Mn_{40.3}Co_{5.7}Sn_{11.2}$ alloy reaches 72.1 J/kg under an applied field changing from 0 to 30 kOe. The external magnetic field shifts the martensitic transition temperature about 3–4 K/10 kOe towards low temperature, indicating that magnetic field can retard the phase transition to a certain extent. The origin of large magnetic entropy change is discussed in the paper.

Keywords: Ni–Mn–Sn, refrigerant capacity, martensitic transition, magnetic entropy change

PACS: 75.30.Sg **DOI:** 10.1088/1674-1056/23/6/067501

1. Introduction

Refrigeration is one of the main sinks of the world electricity consumption and accordingly contributes to worldwide CO_2 emissions. High reduction potentials are envisaged if caloric effects in solid materials are utilized.

In 1997, the discovery of the giant magnetocaloric effect (MCE) at room temperature in $Gd_5Si_2Ge_2$[1] offered a promising development of economical and environmentally-friendly magnetic refrigerant working near room temperature. More recently, the so-called inverse MCE has been observed near room temperature in Ni–Mn–Sn Heusler alloys.[2] Martensitic transformation (MT) is solid-state first-order structural phase transformation, which is displacive, diffusionless, and dominated by the strain-energy arising from shear-like displacements. The recent discovery of giant entropy changes associated with ferroelastic phase transformations promises higher efficiency. Ferroic transitions enhance the entropy change of magneto-, elasto-, baro-, and electro-caloric effects. For better understanding the mechanisms of these materials and also for designing giant MCE materials, a priority program supported by the Deutsche Forschungsgemeinschaft (SPP1599) was established in 2011, which was entitled "Caloric Effects in Ferroic Materials: New Concepts for Cooling".[3]

In the case of Ni_2MnSn alloy, it has a cubic $L2_1$ structure, in which Ni atoms are located at the corner sites, while Mn and Sn atoms are located at the body center sites alternately.[4] In the nonstoichiometric $Ni_2Mn_{1+x}Sn_{1-x}$ alloys, the excess Mn atoms would occupy the vacant Sn sites, and their moments are coupled antiferromagnetically to those of the surrounding Mn atoms on the regular Mn sites.[5] Up to now, most of the researchers have focused on these off-stoichiometric $Ni_2Mn_{1+x}Sn_{1-x}$ alloys, in which the content value of Mn is less than that of Ni. There are few reports about the high-Mn content Mn–Ni–Sn ferromagnetic shape memory alloys (FSMAs),[6,7] in which the content value of Mn is near that of Ni. Moreover, the characteristic temperatures of FSMAs [martensite-start temperature (M_s), martensite-finish temperature (M_f), austenite-start temperature (A_s), and austenite-finish temperature (A_f)] are very sensitive to composition. It was reported that the MT temperatures increased with the increasing of valence electron density (e/a), which was confirmed by the experimental results in Co-, Fe-, Ge-, B-, Al-, Si-, and Cu-doped Ni–Mn–Sn alloys.[8–22]

In this work, the phase transitions and MCE in $Ni_{42.8}Mn_{40.3}Co_{5.7}Sn_{11.2}$ alloy are investigated, a giant magnetic entropy change is obtained, and the influence of external magnetic field on the MT temperature is also examined.

*Project supported by the Natural Science Foundation of Shanxi Province, China (Grant No. 2010011032-1), the Specialized Research Fund for Doctoral Scientific Research of Ministry of Education of China (Grant No. 201014151110003), the Doctoral Scientific Research Foundation of Taiyuan University of Science and Technology, China (Grant No. 20122036), the Postdoctoral Research Station Foundation of Taiyuan University of Science and Technology, China, the Research Project Supported by Shanxi Scholarship Council, China (Grant No. 2013-098), the Graduate Student Innovation Project of Shanxi Province, China (Grant No. 20133114), the National Natural Science Foundation of China (Grant No. 51375325), and the National Key Basic Research Program of China (Grant No. 2012CB722801).

†Corresponding author. E-mail: mgzhang@163.com

© 2014 Chinese Physical Society and IOP Publishing Ltd

2. Experiment

The polycrystalline ingot of $Ni_{42.8}Mn_{40.3}Co_{5.7}Sn_{11.2}$ was prepared by arc melting a required content value of constituent high purity elements (99.98% purity) in a cold copper crucible under an argon atmosphere. For homogenization, the sample was flipped and re-melted. The ingot was cut into small pieces and annealed at 1173 K for 24 h in a vacuum quartz tube, then quenched in ice water. Microstructure and elemental composition of the sample were investigated by field emission scanning electron microscopy (FE-SEM) (Hitachi S-4800) attached with an x-ray energy dispersive spectroscopy (EDS) (Thermo System 7) setup. The crystal structure of the sample was analyzed by using PANalytical X'Pert PRO type X-ray diffractometer with Cu $K\alpha$ radiation at room temperature. The magnetic properties were measured by using a Quantum Design's multi-use vibrating sample magnetometer VersaLab system under a magnetic field up to 30 kOe. The temperature-dependent magnetization (M–T) curves were measured at cooling/heating rate of 3 K/min. Instrument temperature measurement range was between 50 K–400 K.

3. Results and discussion

Figure 1 shows XRD pattern of $Ni_{42.8}Mn_{40.3}Co_{5.7}Sn_{11.2}$ alloy at room temperature. The diffraction peaks in the alloy are indexed. All the peaks correspond to the $L2_1$ cubic structure, which indicates that the sample is in austenitic phase and the MT temperature is below room temperature.

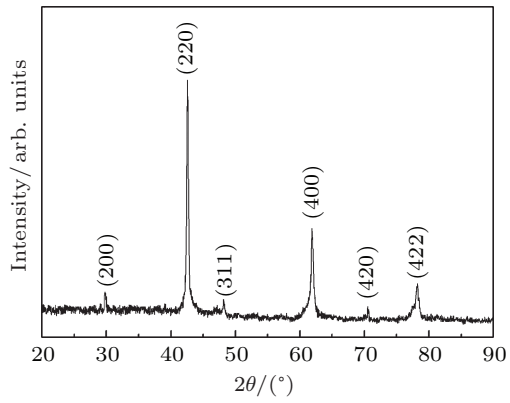


Fig. 1. The XRD pattern of $Ni_{42.8}Mn_{40.3}Co_{5.7}Sn_{11.2}$ alloy at room temperature.

The temperature-dependent magnetization (M–T) curves for the $Ni_{42.8}Mn_{40.3}Co_{5.7}Sn_{11.2}$ alloy is measured. Figure 2 shows the M–T curves for $Ni_{42.8}Mn_{40.3}Co_{5.7}Sn_{11.2}$ on heating and cooling in magnetic fields of 10 kOe and 1 kOe respectively. As shown in Fig. 2(a), the sample was measured in zero-field-cooled mode (ZFC) from above the Curie temperature of austenitic phase (T_C^A) down to the target temperature. Figure 2(b) shows a thermal hysteresis about 15 K around the MT temperature, while no thermal hysteresis is observed near T_C^A. Between the MT and the reverse MT, there is an obvious thermal hysteresis, which is attributed to the first-order structural transition. The values of M_s, M_f, A_s, and A_f are estimated from M–T curves to be 204, 192, 206, and 220 K, respectively. In the Ni–Mn-based Heusler alloys, the exchange interactions are of long range and of an indirect Ruderman–Kittel–Kasuya–Yosida-type.[7] Besides the variations of the e/a (e/a is the valence electron concentrations per atom, determined by the concentration-weighted sum of s, d, and p electrons) in these alloys, it is reported that in the Ni–Mn-based Heusler alloys, the exchange interactions, and consequently, magnetic ordering temperatures are also sensitive to Mn–Mn distance.[5] In the $Ni_{42.8}Mn_{40.3}Co_{5.7}Sn_{11.2}$ alloy, the lattice contraction may modify the Mn–Mn distance and also influence the MT temperature and T_C^A.

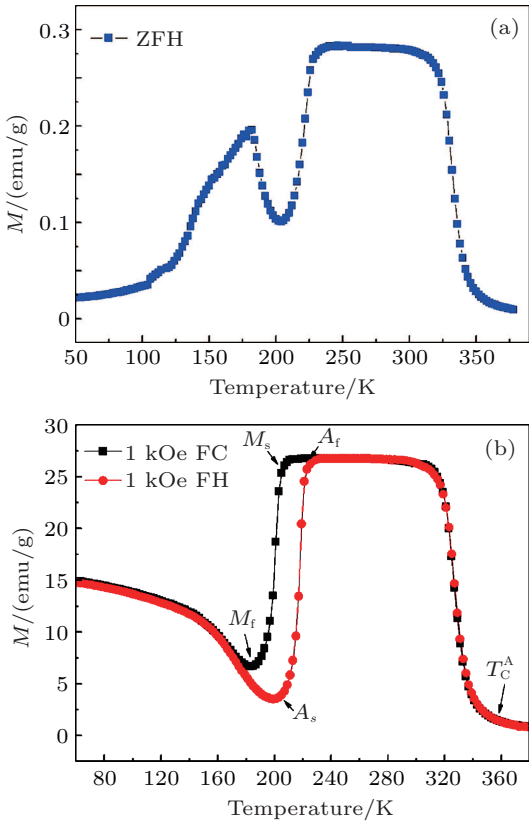


Fig. 2. (color online) The M–T curves for $Ni_{42.8}Mn_{40.3}Co_{5.7}Sn_{11.2}$ alloy heated under a magnetic field 10 Oe (a); heated (FH) and cooled (FC) under a magnetic field of 1 kOe (b).

The isothermal magnetization curves (M–H) for the $Ni_{42.8}Mn_{40.3}Co_{5.7}Sn_{11.2}$ alloy are measured around MT temperature and T_C^A temperature. Figure 3(a) shows the M–H curves for $Ni_{42.8}Mn_{40.3}Co_{5.7}Sn_{11.2}$ with a field increasing from zero up to 30 kOe. The typical metamagnetic behavior, due to the field-induced MT, can be observed in these plots. The magnetization difference reaches 62 emu/g, within the temperature changes of about 12 K. The magnetization jump in FSMA would be attributed to two different interaction mechanisms. One mechanism may be the strong spin-

phonon coupling, resulting in a difference in magnetic state between the austenitic phase and the martensitic phase. The other mechanism is due to the magnetostructural coupling on a mesoscopic scale between the magnetism and the martensitic variants, which leads to the magnetization jump near MT. The metamagnetic characteristic in the M–H isotherm is associated with a field-induced reverse MT from a low magnetization martensitic state to a higher magnetization austenite state. This phenomenon has been reported in magnetic field-induced MT in the other Ni–Mn-based FSMAs.[15] Figure 3(b) shows the M–H curves for $Ni_{42.8}Mn_{40.3}Co_{5.7}Sn_{11.2}$ around the T_C^A temperature, indicating the typical magnetic property changes near the Curie temperature.

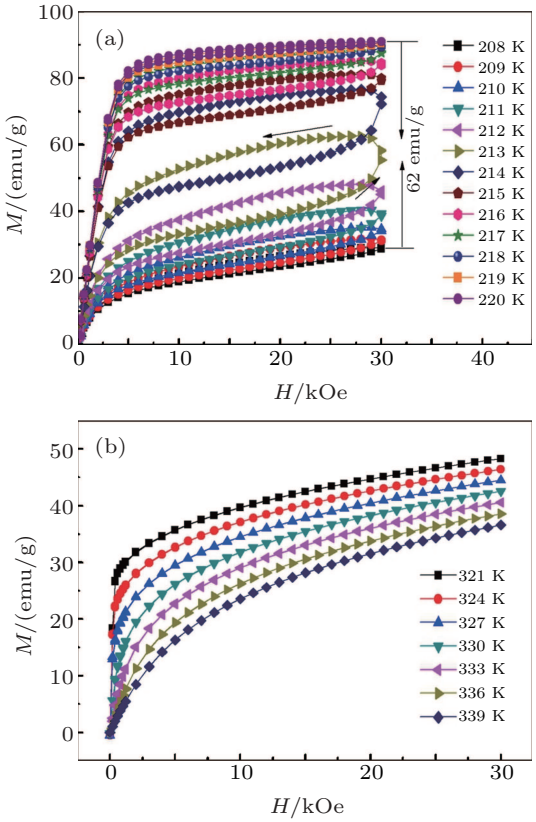


Fig. 3. (color online) The isothermal magnetization curves (M–H) of $Ni_{42.8}Mn_{40.3}Co_{5.7}Sn_{11.2}$ alloy measured at various temperatures: (a) around MT temperature, (b) around T_C^A temperature.

As is well known, the Arrott plot, which is obtained by plotting M^2 versus H/M, is an effective tool for identifying the order of phase transition.[23] If the slope of the plot is negative, the magnetic transition will be of the first-order. On the other hand, it is expected to be the second-order when the slope is positive. Figure 4(a) shows the Arrott plots for the sample $Ni_{42.8}Mn_{40.3}Co_{5.7}Sn_{11.2}$ around its MT temperature. It is clear that S-shaped curves are observed at 213 K and 214 K, suggesting the occurrence of a field-induced first-order phase transition. This should be attributed to the coherent coupling between the spin and the lattice system.[24] Figure 4(b) shows the Arrott plots for the sample $Ni_{42.8}Mn_{40.3}Co_{5.7}Sn_{11.2}$ around its T_C^A temperature, indicating a typical second-order phase transition.

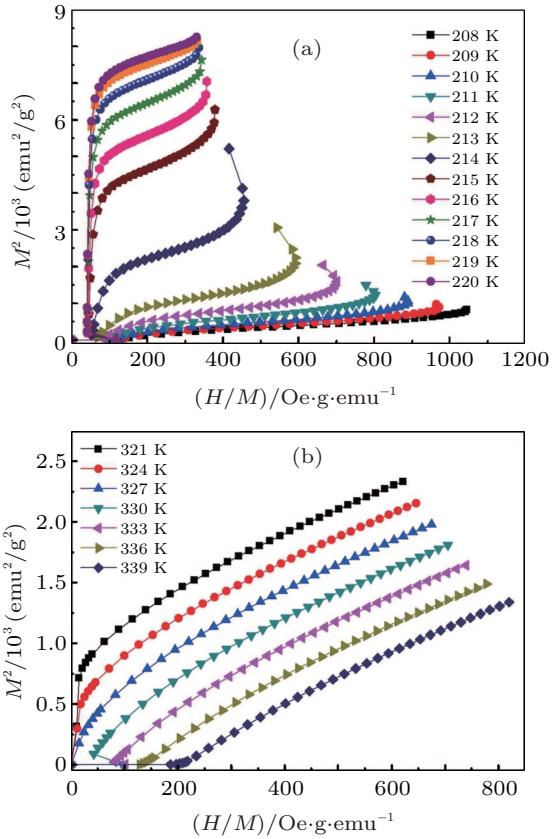


Fig. 4. (color online) Arrott plots for $Ni_{42.8}Mn_{40.3}Co_{5.7}Sn_{11.2}$ alloy (a) around MT temperature and (b) around T_C^A temperature.

Owing to the large and sharp changes in magnetization associated with the MT, large MCE would be expected in $Ni_{42.8}Mn_{40.3}Co_{5.7}Sn_{11.2}$ alloy. The ΔS_M as a function of temperature and magnetic field for the alloy is calculated from isothermal magnetization curves by using the Maxwell equation:[2,15]

$$\Delta S_M(T,H) = \int_0^H \left(\frac{\partial M(T,H)}{\partial T}\right)_H \mathrm{d}H.$$

The temperature dependences of ΔS_M in applied fields (ΔH) of 10, 20, and 30 kOe for $Ni_{42.8}Mn_{40.3}Co_{5.7}Sn_{11.2}$ are shown in Fig. 5. Around the MT temperature, the maximum value of ΔS_M is 45.6 J/kg·K for the applied field of 30 kOe. Even at ΔH of 10 kOe, we still have a ΔS_M of 14.2 J/kg·K. As shown in Fig. 5(b), the peak values of ΔS_M around T_C^A reach -1.2 J/kg·K, -2.0 J/kg·K, and -2.8 J/kg·K for ΔH of 10, 20, and 30 kOe, respectively. The refrigerant capacity (RC) is also an important parameter to evaluate MCE, which is a measurement of the heat transferred between the cold and hot reservoirs in an ideal refrigeration cycle.[25,26] RC values are usually determined by numerically integrating the ΔS_M–T curves over the full width at half maximum. With the field changing from 0 to 30 kOe, the RC value around the MT of $Ni_{42.8}Mn_{40.3}Co_{5.7}Sn_{11.2}$ alloy reaches 106.9 J/kg.

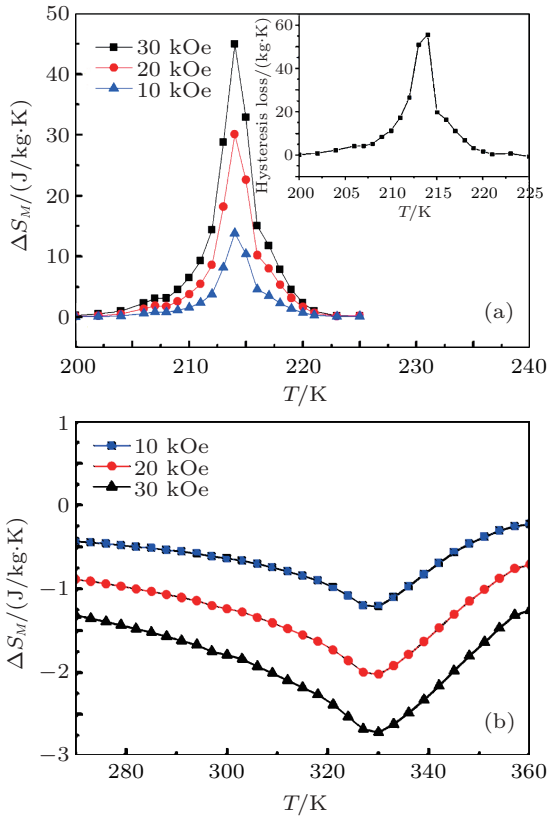


Fig. 5. (color online) Temperature dependences of ΔS_M in the magnetic fields of 10, 20, and 30 kOe for $Ni_{42.8}Mn_{40.3}Co_{5.7}Sn_{11.2}$ alloy at first-order transition (a), and the second-order transition (b).

It is worth noting that hysteresis loss exists around first-order magnetic transition and should be taken into account in the evaluation of RC. Here, the hysteresis losses at different temperatures are estimated from the enclosed area between the magnetizing and demagnetizing M–H curves as shown in the inset of Fig. 5(a). The average hysteresis loss for the alloy is calculated by integrating the area under the curve of hysteresis loss versus temperature using the same temperature range as that in calculation of RC, which serves as the integration limit.[27] For the $Ni_{42.8}Mn_{40.3}Co_{5.7}Sn_{11.2}$ alloy, the average hysteresis loss is determined to be 34.8 J/kg, lower than that observed in the other Heusler alloys.[28,29] Therefore, the effective RC can be evaluated by subtracting the average hysteresis loss from RC for these alloys. If the hysteresis loss is taken into account, the effective RC value around MT for the $Ni_{42.8}Mn_{40.3}Co_{5.7}Sn_{11.2}$ alloy is found to be 72.1 J/kg, which is comparable to those in other Ni–Mn-based Heusler alloys.[27–29] For the second-order transition, the RC value calculated from Fig. 5(b) reaches −160.1 J/kg with the field changing from 0 to 30 kOe. Therefore, the value of RC around the second-order transition is larger than that around the first-order transition.

In order to better study the influence of applied magnetic field on the MT of the alloy, the MT temperatures at different applied magnetic fields have been tested. Figure 6 shows the M–T curves for $Ni_{42.8}Mn_{40.3}Co_{5.7}Sn_{11.2}$ alloy on heating and cooling under the fields of 10, 20, and 30 kOe, respectively. The different external magnetic fields exert important influences on the phase transition temperature. Although the M–T curves of 10, 20, and 30 kOe are similar to that of 1 kOe, it can be clearly seen that the jump in magnetization is significantly shifted towards low temperature with the increase of magnetic field, and all the characteristic temperatures of MT shift down about 10 K as magnetic field increases from 10 kOe to 30 kOe. The field dependence of MT temperature suggests that magnetic field can compete with temperature in affecting the phase transition.[24]

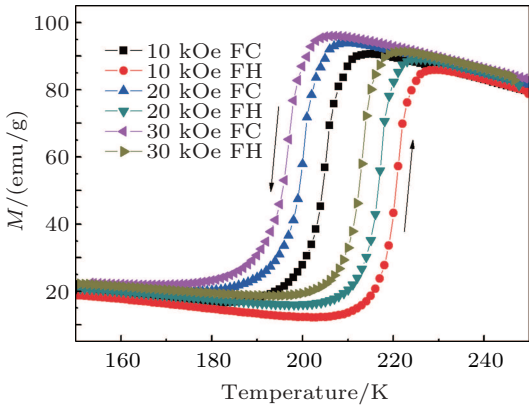


Fig. 6. (color online) The M–T curves for $Ni_{42.8}Mn_{40.3}Co_{5.7}Sn_{11.2}$alloy on heating and cooling under magnetic fields of 10, 20, and 30 kOe.

4. Conclusion

The component dependence of MT and ΔS_M in $Ni_{42.8}Mn_{40.3}Co_{5.7}Sn_{11.2}$ alloy is investigated. A large magnetic entropy change of 45.6 J/kg·K around the MT at 30 kOe is obtained. With the field changing from 0 to 30 kOe, the effective RC values of $Ni_{42.8}Mn_{40.3}Co_{5.7}Sn_{11.2}$ alloy are 72.1 J/kg around the first-order transition temperature and 160.1 J/kg at the second-order transition temperature. The large magnetic entropy change can be ascribed to the abrupt change of magnetization in the vicinity of MT temperature. The giant ΔS_M, large effective RC, and the low cost suggest that $Ni_{42.8}Mn_{40.3}Co_{5.7}Sn_{11.2}$ alloy is a promising working substance for magnetic refrigeration.

References

[1] Pecharsky V K and Gschneidner K A Jr 1997 *Phys. Rev. Lett.* **78** 4494
[2] Krenke T, Duman E, Acet M, Wassermann E F, Moya X, Mañosa L and Planes A 2005 *Nat. Mater.* **4** 450
[3] http://wwwferroiccoolingde/
[4] Xuan H C, Wang D H, Zhang C L, Han Z D, Gu B X and Du Y W 2008 *Appl. Phys. Lett.* **92** 102503
[5] Sutou Y, Imano Y, Koeda N, Omori T, Kainuma R, Ishida K and Oikawa K 2004 *Appl. Phys. Lett.* **85** 4358
[6] Xuan H C, Zheng Y X, Ma S C, Cao Q Q, Wang D H and Du Y W 2010 *J. Appl. Phys.* **108** 103920
[7] Wu Z G, Liu Z H, Yang H, Liu Y N and Wu G H 2011 *Intermetallics* **19** 1839
[8] Krenke T, Duman E, Acet M, Moya X, Manosa L and Planes A 2007 *J. Appl. Phys.* **102** 033903

[9] Aksoy S, Krenke T, Acet M, Wassermann E F, Moya X, Mañosa L and Planes A 2007 *Appl. Phys. Lett.* **91** 241916
[10] Hu F X, Shen B G and Sun J R 2013 *Chin. Phys. B* **22** 037505
[11] Dincer I, Yüzüak E and Elerman Y 2010 *J. Alloys Compd.* **506** 508
[12] Liu Z H, Wu Z G, Yang H, Liu Y N, Wang W H, Ma X Q and Wu G H 2011 *Intermetallics* **19** 1605
[13] Li Z, Jing C, Zhang H L, Qiao Y F, Cao S X, Zhang J C and Sun L 2009 *J. Appl. Phys.* **106** 083908
[14] Nayak A K, Suresh K G and Nigam A K 2010 *J. Appl. Phys.* **107** 09A927
[15] Han Z D, Wang D H, Zhang C L, Xuan H C, Zhang J R, Gua B X and Du Y W 2009 *Mater. Sci. Eng. B* **157** 40
[16] Sharma V K, Chattopadhyay M K and Roy S B 2010 *J. Phys. D: Appl. Phys.* **43** 225001
[17] Wang R L, Yan J B, Xiao H B, Xu L S, Marchenkov V V, Xu L F and Yang C P 2011 *J. Alloys Compd.* **509** 6834
[18] Chen J, Han Z D, Qian B, Zhang P, Wang D H and Du Y W 2011 *J. Magn. Magn. Mater.* **323** 248
[19] Yüzüak E, Emre B, Elerman Y and Yücel A 2010 *Chin. Phys. B* **19** 057501
[20] Shen J, Li Y X, Dong Q Y, Wang F and Sun J R 2008 *Chin. Phys. B* **17** 2268
[21] Ma S C, Wang D H, Xuan H C, Shen L J, Cao Q Q and Du Y W 2011 *Chin. Phys. B* **20** 087502
[22] Tegus O, Bao L H and Song L 2013 *Chin. Phys. B* **22** 037506
[23] Arrott A 1957 *Phys. Rev.* **108** 1394
[24] Anzai S and Ozawa K 1978 *Phys. Rev. B* **18** 2173
[25] Gschneidner K A Jr, Pecharsky V K, Pecharsky A O and Zimm C B 1999 *Mater. Sci. Forum* **315** 69
[26] Gschneidner K A Jr, Pecharsky V K and Tsokol A O 2005 *Rep. Prog. Phys.* **68** 1479
[27] Hernando B, Llamazares J L S, Prida V M, Baldomir D, Serantes D, Ilyn M and González J 2009 *Appl. Phys. Lett.* **94** 222502
[28] Pathak A K, Dubenko I, Karaca H E, Stadler S and Ali N 2010 *Appl. Phys. Lett.* **97** 062505
[29] Pathak A K, Khan M, Dubenko I, Stadler S and Ali N 2007 *Appl. Phys. Lett.* **90** 262504